Supporting Information

DNA-Guided Plasmonic Helix with Switchable Chirality

Xiang Lan,[1,2] Tianji Liu,[3,4] Zhiming Wang,[4] Alexander O. Govorov,[3] Hao Yan,[1,2] Yan Liu[1,2]

[1]Center for Molecular Design and Biomimetics, The Biodesign Institute, Arizona State University, Tempe, AZ 85287, USA

[2]School of Molecular Sciences, Arizona State University, Tempe, AZ 85287, USA

[3]Department of Physics and Astronomy, Ohio University, Athens, Ohio 45701, USA

[4]Institute of Fundamental and Frontier Sciences, University of Electronic Science and Technology of China, Chengdu 610054, China

Note S1. Experimental methods

Basically, we followed our previously-published protocols[1] for self-assembly of DNA origami, conjugation of gold nanorods to DNA origami, self-assembly of gold nanorod superstructures and CD measurements. Table S1 presents the detailed annealing procedures for different experiment steps in this work.

Table S1. Annealing conditions for different steps of experiment.

Experiment	**Temperature**	**Rate**	**Cycle**
Self-assembly of DNA origami	From 65 °C to 25 °C	1 h/°C	NA
Attachment of AuNRs onto DNA origami	From 45 °C to 30 °C	10 min/°C	4
Self-assembly of AuNR superstructures	From 45°C to 30 °C	3 h/°C	NA
Reconfiguration 1	From 45 °C to 30 °C	1 h/°C	NA
Reconfiguration 2	From 37 °C to 25 °C	10 min/°C	4

Reconfiguration 1 is for the conversion of AuNR superstructure between the folded state and the extended state.
Reconfiguration 2 is for the chirality inversion of the AuNR superstructure.

Table S2. Plasmon treatments for different hydrophilicities of the TEM grid surface.

Surface	**Current /mA**	**Time /s**	**Membrane**
Strong charge	45	30	Formvar
Weak charge	30	20	Carbon

Table S3. Condition for obtaining a negative or positive staining of the DNA structures.

UF staining	**Negative**	**Positive**
Aqueous layer	With	Without

Aqueous layer means that a thin layer of 2% uranyl formate solution was left on the TEM grid surface after staining for 30 s.

Note S2. Simulation techniques

Extinction and CD spectra were obtained by utilizing a commercial software package (FDTD solutions, Lumerical Inc.). Using a perfectly matched layer (PML) as the boundary conditions, the CD spectra were respectively calculated and averaged in the ±x, ±y, and ±z directions. Balancing the need for accuracy in the calculations with computational time and memory requirements, the mesh sizes were specified as 1 nm in the x, y, and z directions. To better address the curved surface of the AuNR, the mesh sizes were further refined with the Yu-Mittra method[2]. Additionally, due to the inhomogeneous broadening effect that originated from the polydispersity in the superstructures, the dielectric function of the Au was modified and followed the methods used in our previous approach[3]:

$$\varepsilon_{\mathrm{Au}}(\omega) = \varepsilon_{bulk\ \mathrm{Au}}(\omega) + \frac{\omega_p^2}{\omega^2 + i\omega\Gamma_{bulk\ \mathrm{Au}}} - \frac{\omega_p^2}{\omega^2 + i\omega\Gamma_{bulk\ \mathrm{Broadened}}} \quad , \tag{1}$$

where $\varepsilon_{bulk\ \mathrm{Au}}(\omega)$ denotes the frequency-dependent complex permittivity of bulk gold and the values were taken from the tabulated data[4]. $\Gamma_{bulk\ \mathrm{Au}}$ = 0.076 eV and ω_p = 8.9 eV were fitting parameters in the Drude model[5]. $\Gamma_{bulk\ \mathrm{Broadened}} = 5\ \Gamma_{bulk\ \mathrm{Au}}$ was a broadened damping parameter that was obtained by fitting the results with the experimental extinction spectra of the individual AuNR.

Note S3. Additional TEM images of self-assembled AuNR chiral superstructures

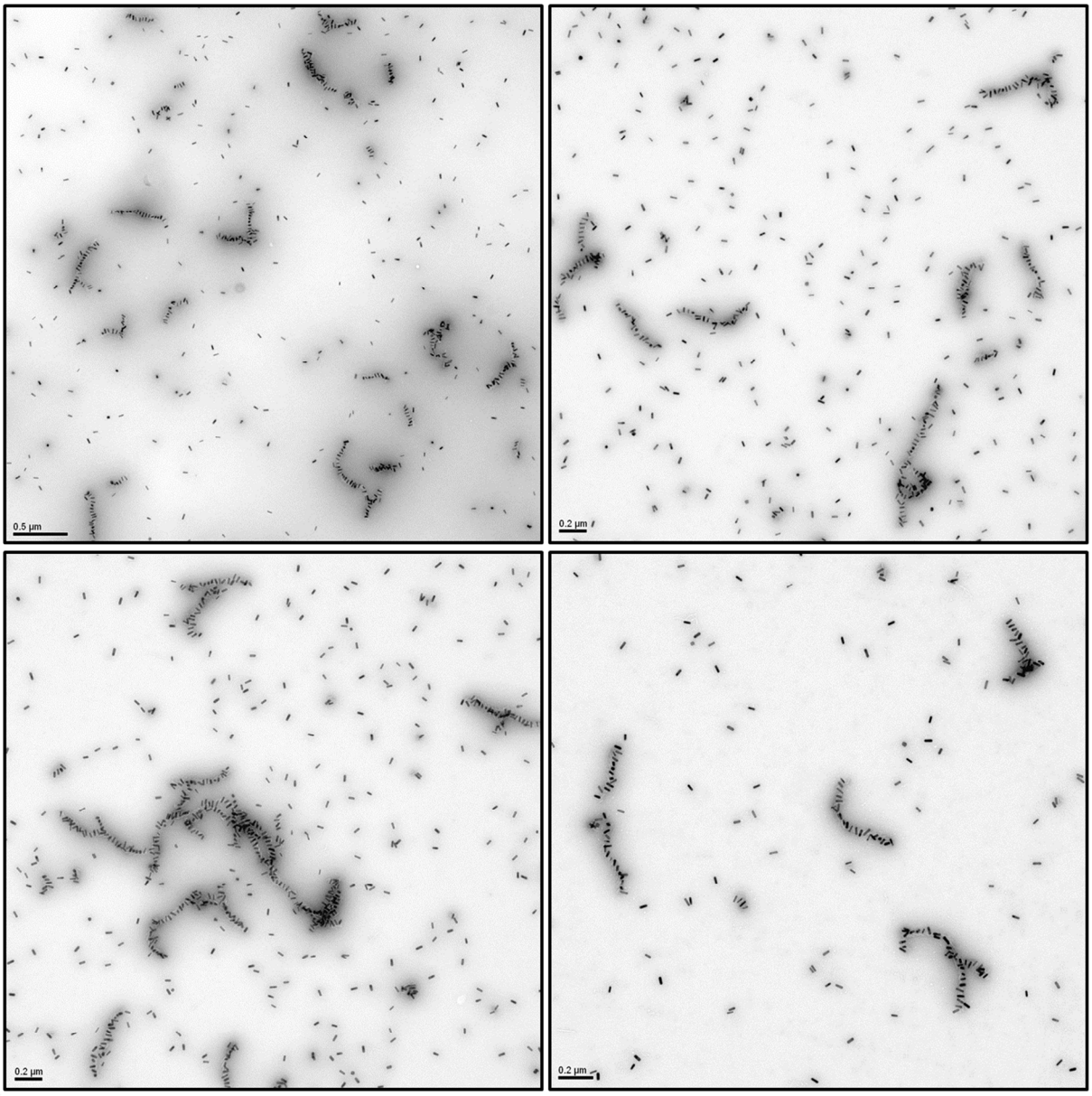

Figure S1. Wide field TEM images of left-handed AuNR superstructures. DNA origami in the folded state that are used for the assembly process.

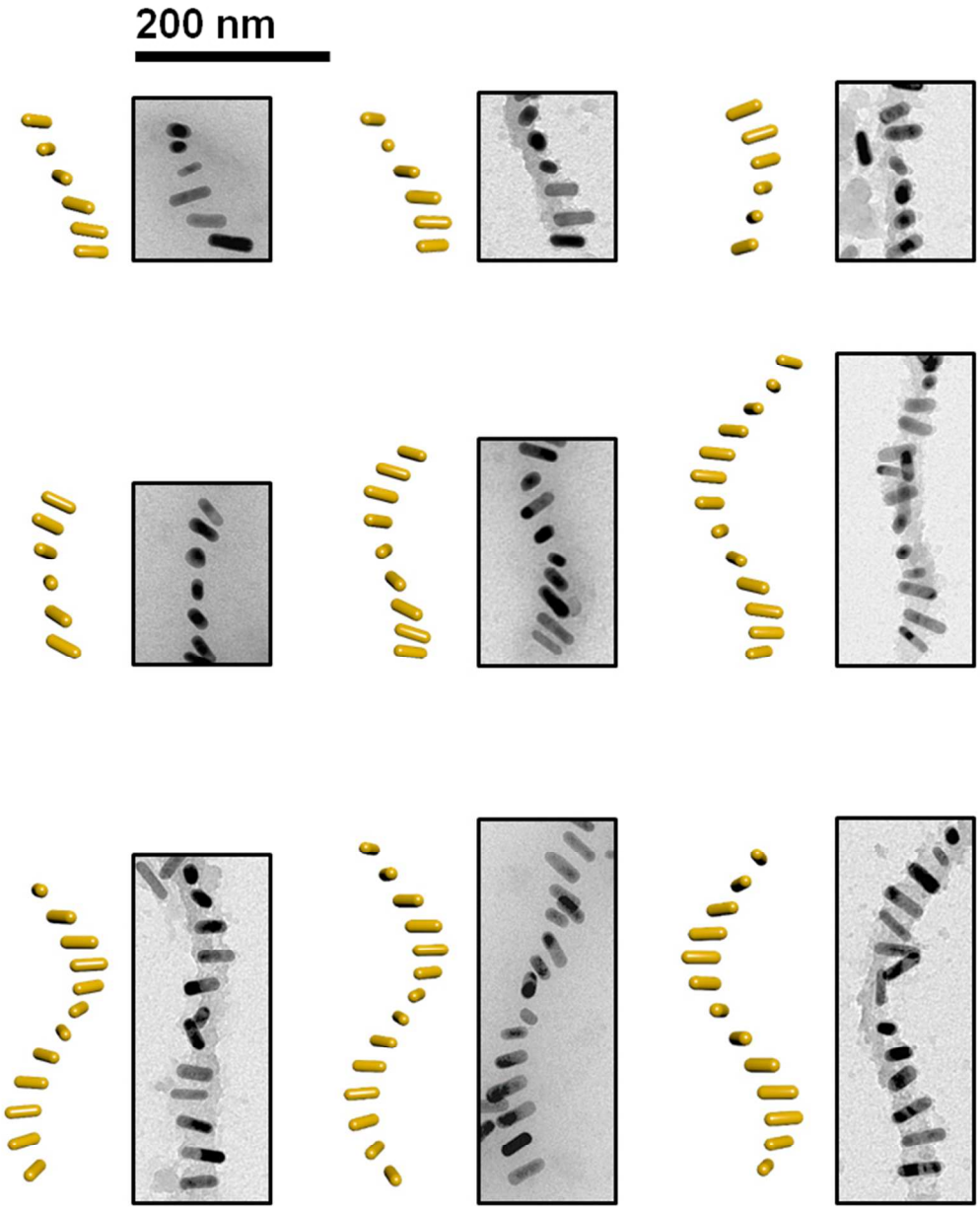

Figure S2. Zoomed-in TEM images of individual AuNR superstructures and the corresponding 3D models that have a similar spatial orientation. DNA origami in the folded state was used during the assembly process.

Note S4. TEM characterization of monomeric and polymeric DNA origami

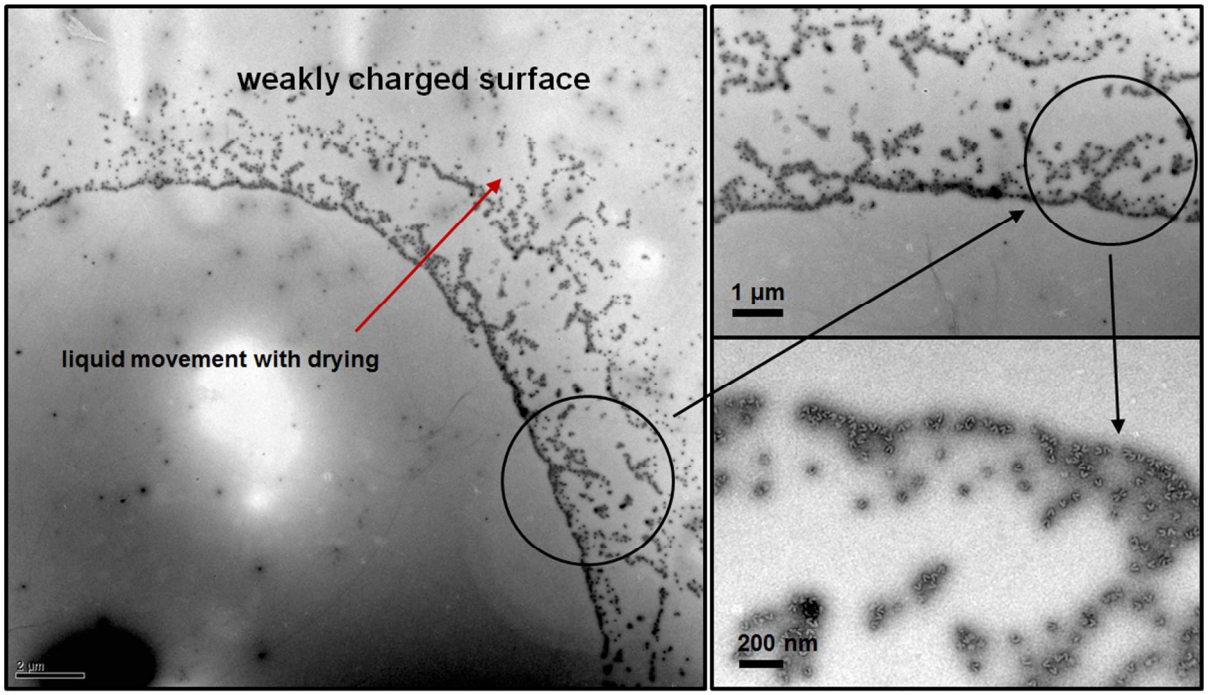

Figure S3. These TEM images show the liquid movement while the sample deposited on the surface of a weakly-charged TEM grid was drying. The weak wettability of the surface was due to the low hydrophilicity. The DNA origami prefer to stand up with the ends of the helices in contact with the TEM grid surface.

In this work, the DNA origami (both V-shape and H-shape) has 3 layers of parallel DNA double helix in each arm. The helical ends that have single-stranded scaffold loops are relatively more hydrophobic than the helical sides because of the exposure of the DNA bases. The hydrophobic interactions between DNA blunt ends have been demonstrated in high ion concentrations or at low temperatures.[6]

In our case, although the DNA origami have weak hydrophobic interactions between each other because of the relatively low ion concentrations (~ 6 mM Mg^{2+}), the hydrophobicity differences between the helical ends and sides of DNA origami still greatly influence the attachments of the DNA origami on TEM grid surfaces with different treatments, such as glow discharging of the formvar or carbon film (Table S2). The helical sides of the DNA origami with more hydrophilicity were preferentially attached to the strongly charged surfaces (formvar), while the helical ends of the DNA origami with more hydrophobicity were more likely attached to the weakly charged surfaces (carbon). Overall, it is the hydrophilicity variations between the helical sides and helical ends that dominates the different preference of DNA origami attachments on TEM grid surfaces.

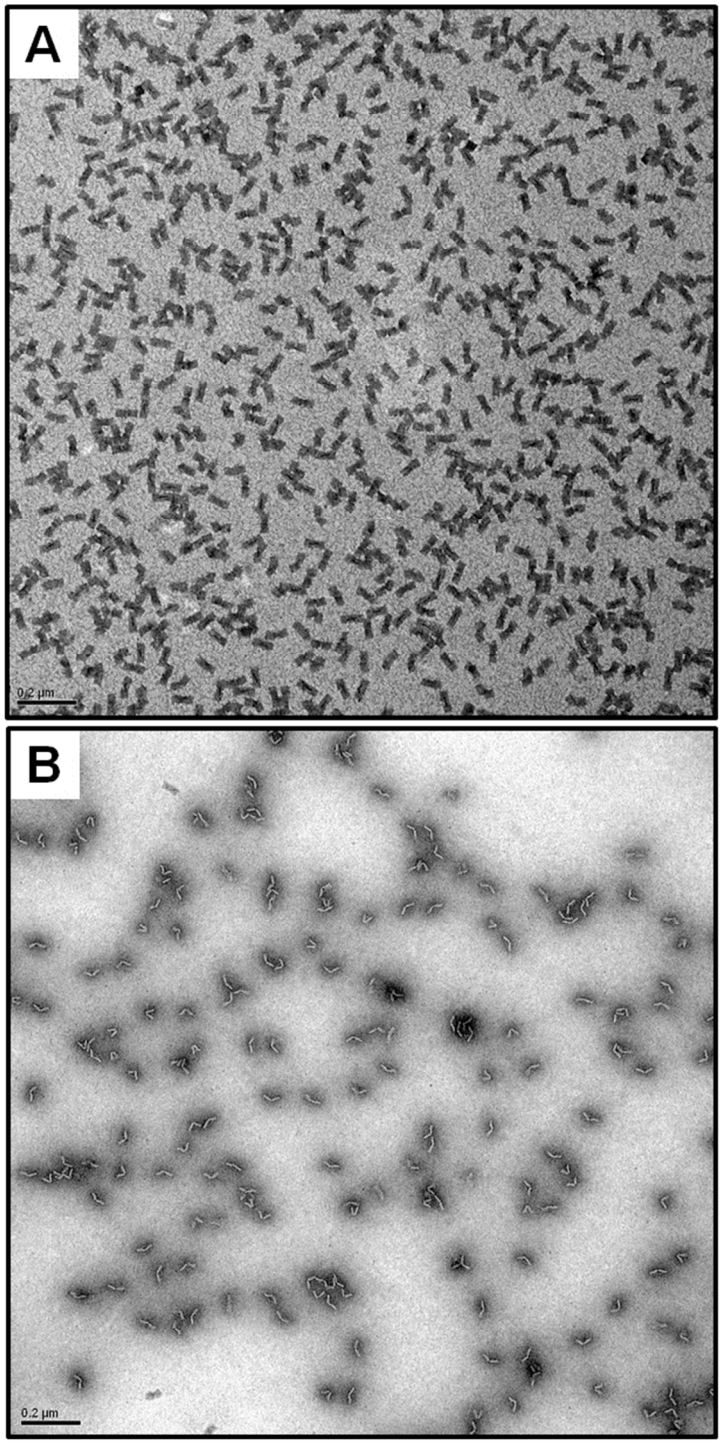

Figure S4. The differential attachments of DNA origami on strongly-charged (A) and weakly-charged (B) TEM grid surfaces, respectively. DNA origami in the extended state that were transformed from the folded state are presented here. On the strongly charged grid surface, the DNA origami prefer to lie down with the flat surface of the DNA helical bundle in contact with the surface, while on the weakly charged grid surface, they prefer to stand up with the ends of the DNA helices in contact with the surface.

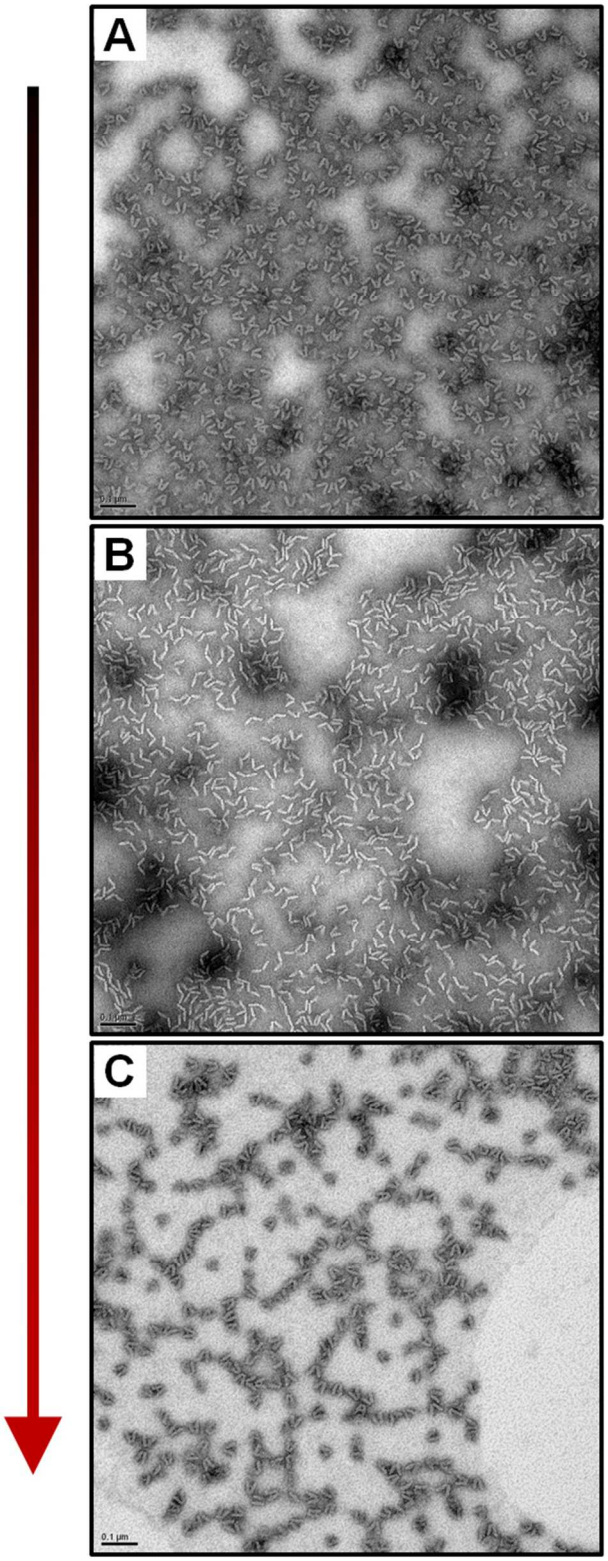

Figure S5. A full cycle of structural reconfiguration. The DNA origami's structure was cycled from the folded state to the extended state and back to the folded state.

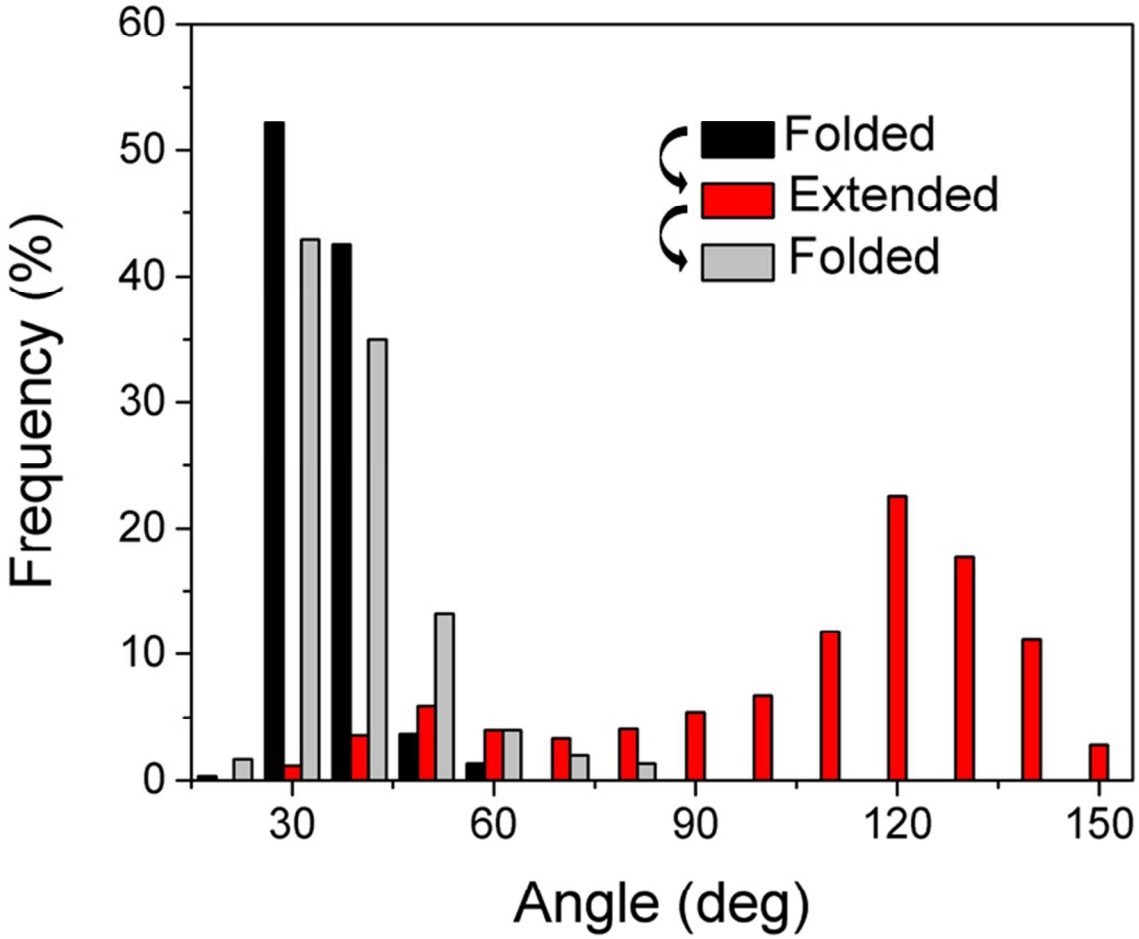

Figure S6. Histograms of the inter-arm angle of the DNA origami for a full cycle of conversion between the folded state and the extended state. The yield of the structural conversion was not 100% and some intermediate states were present. 300 and 1000 particles were counted for the folded state and the extended state, respectively.

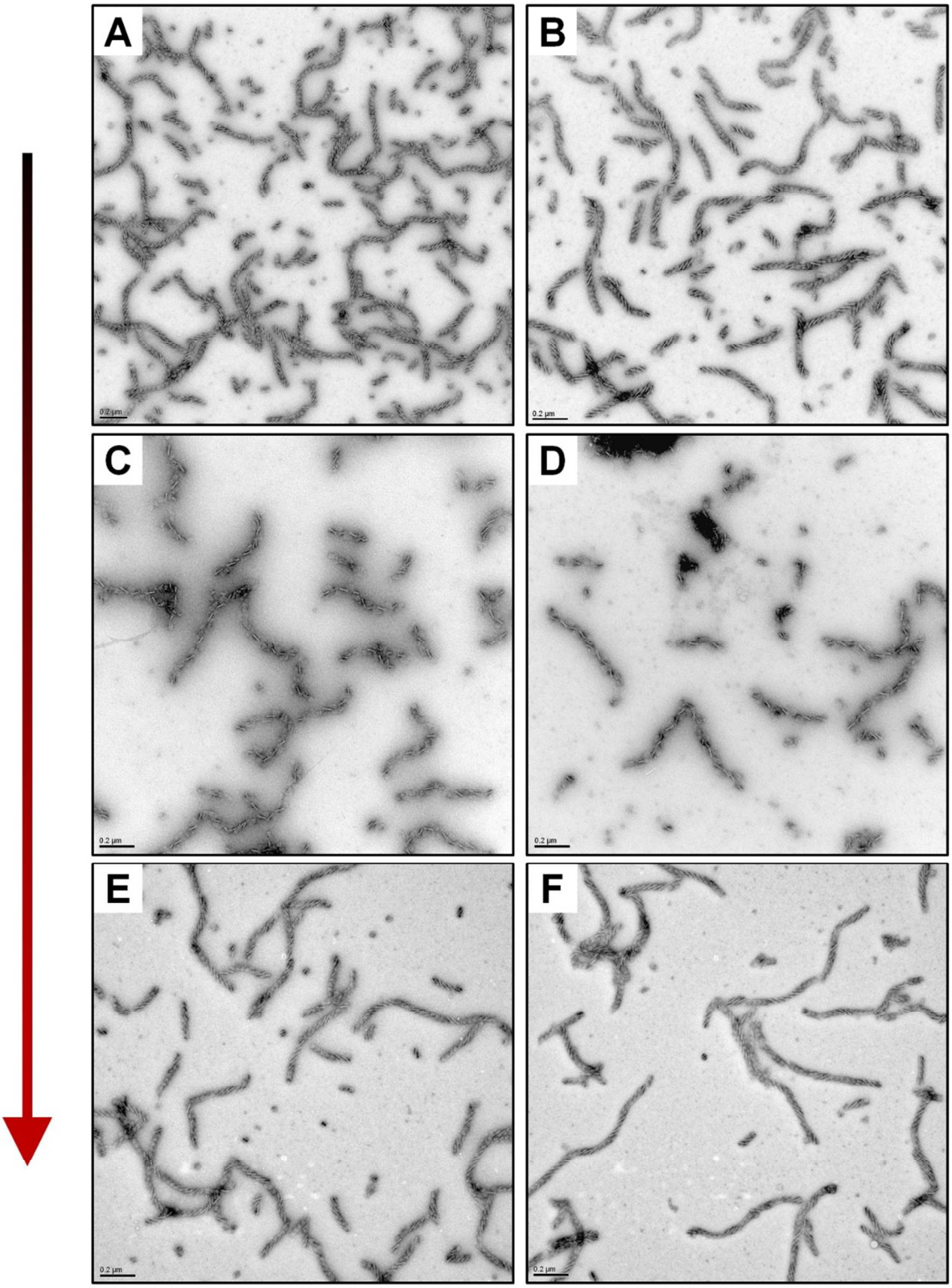

Figure S7. These TEM images show a full cycle of DNA origami supramolecular polymer structural reconfiguration. This conversion allowed the DNA origami to change from the folded state to the extended state and back to the folded state. A, B, E, F) the folded state; C, D) the extended state.

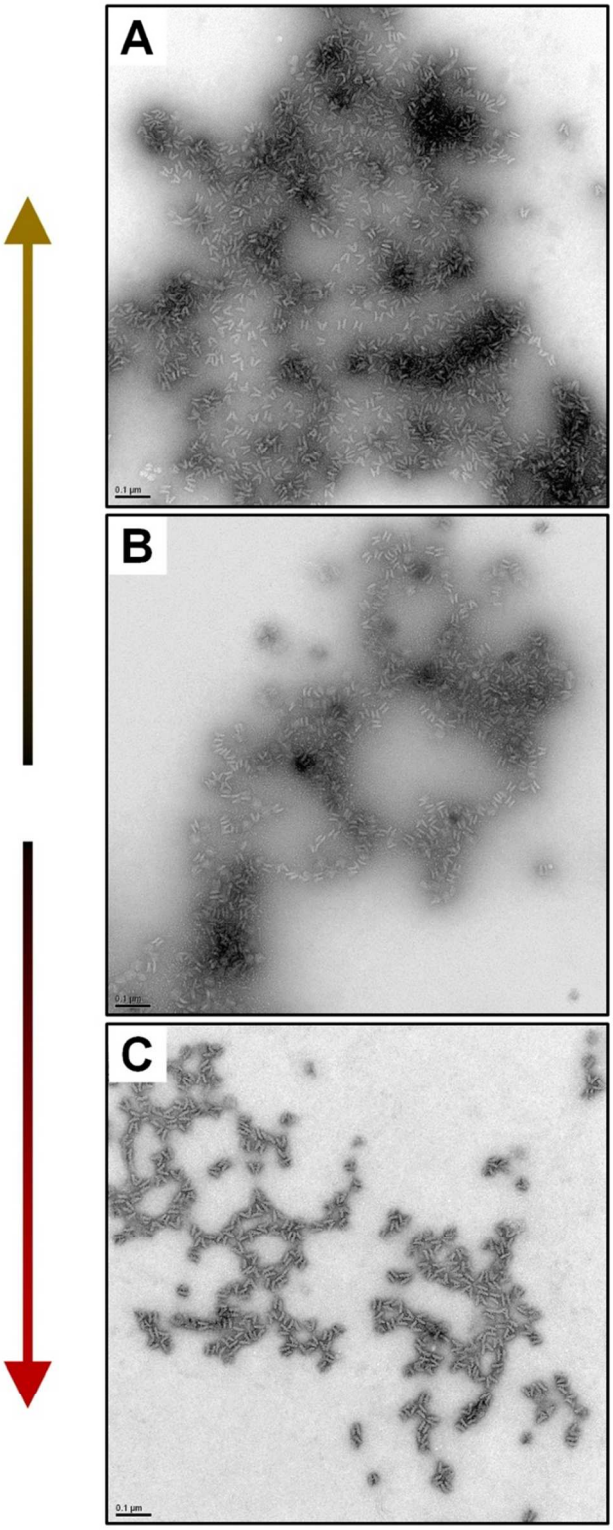

Figure S8. The structural reconfiguration from H-shaped origami (B) to two mirror-image V-shaped structures in (A) and (C). A) The monomeric DNA origami that were used for the self-assembly procedures for the left-handed superstructures; C) The monomeric DNA origami that were used for the self-assembly of the right-handed superstructures.

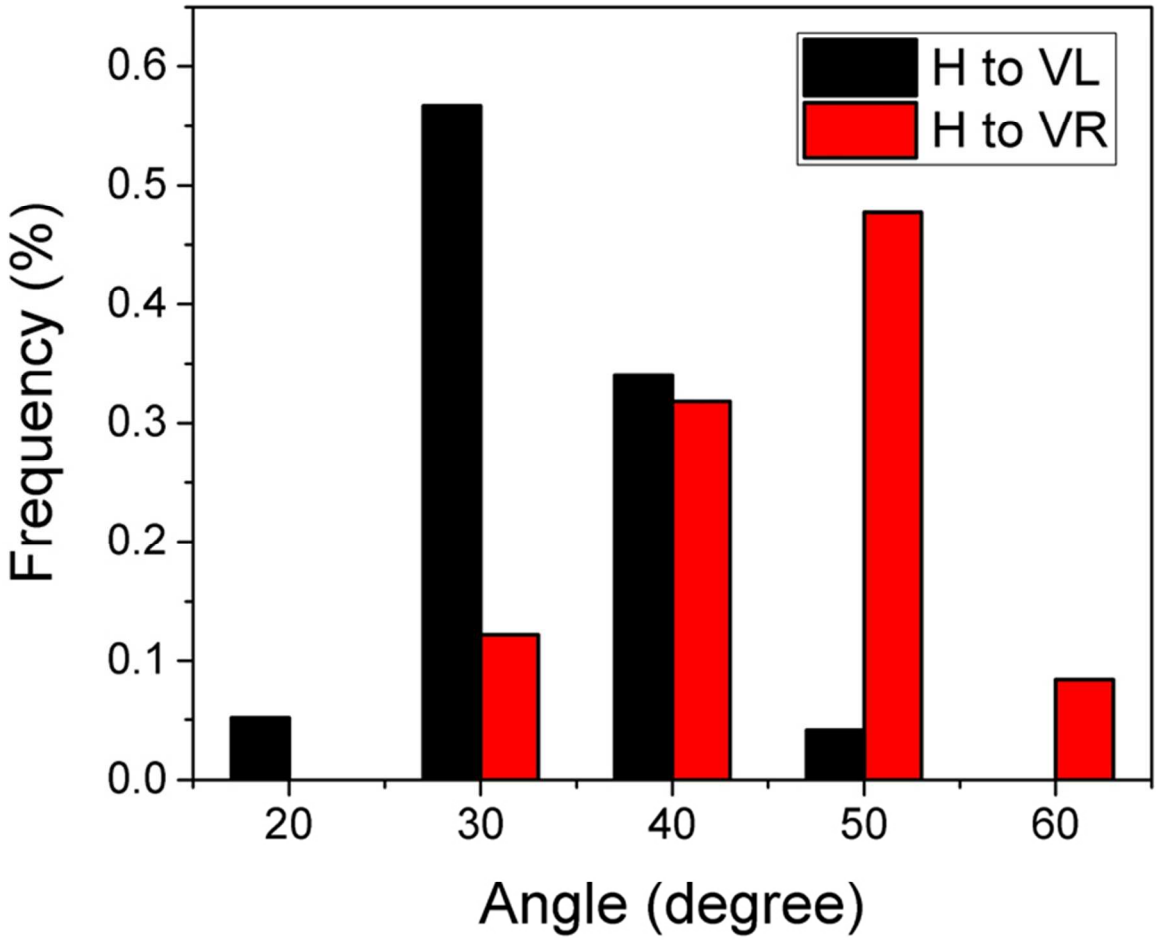

Figure S9. Histograms of the inter-arm angle of two V-shaped structures that were transformed from the H-shaped DNA origami. VL and VR denote the monomeric DNA origami for the corresponding left-handed and right-handed superstructures, respectively. 300 particles were counted for both VL and VR.

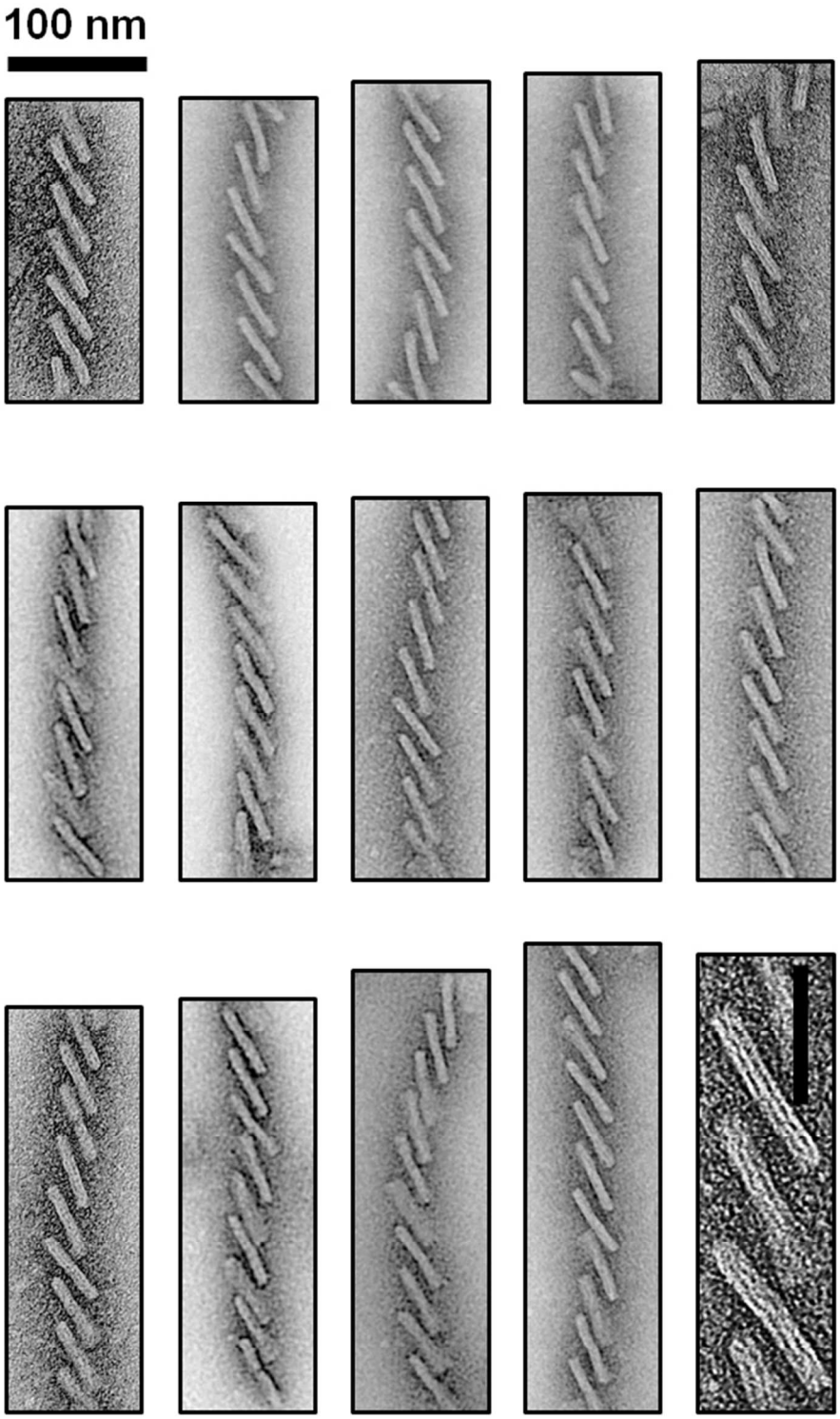

Figure S10. A collection of DNA superstructures that were assembled from H-shaped DNA origami monomers. The scale bar in the bottom-right image is 50 nm.

Note S5. Experimental absorption spectra of AuNR superstructures

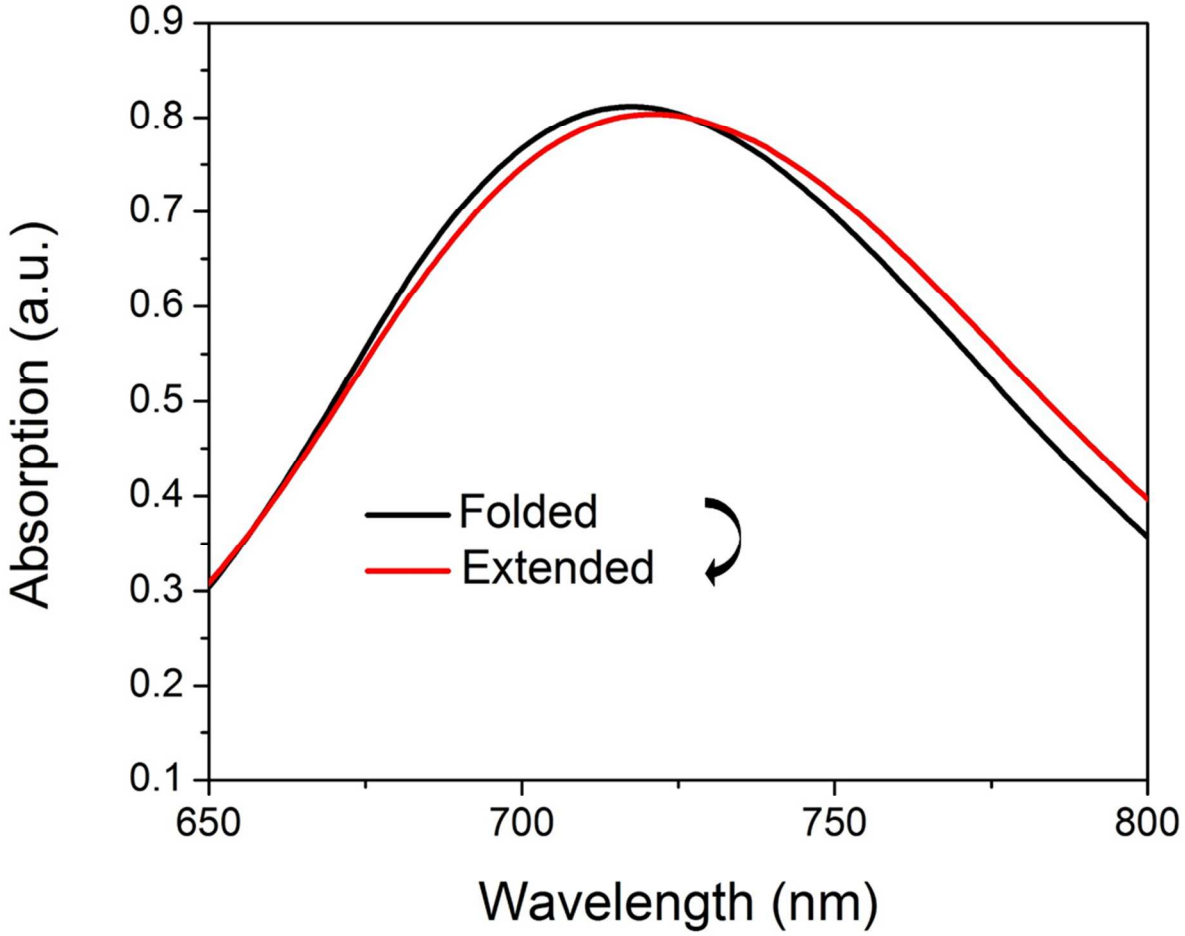

Figure S11. The experimental absorption spectra change after a single step reconfiguration of the AuNR superstructures from the folded state to the extended state. A spectral red shift is observed because the dominant plasmon modes was changed from that of an anti-bonding to a bonding mode after the structural reconfiguration. No apparent aggregation was observed from the absorption spectra.

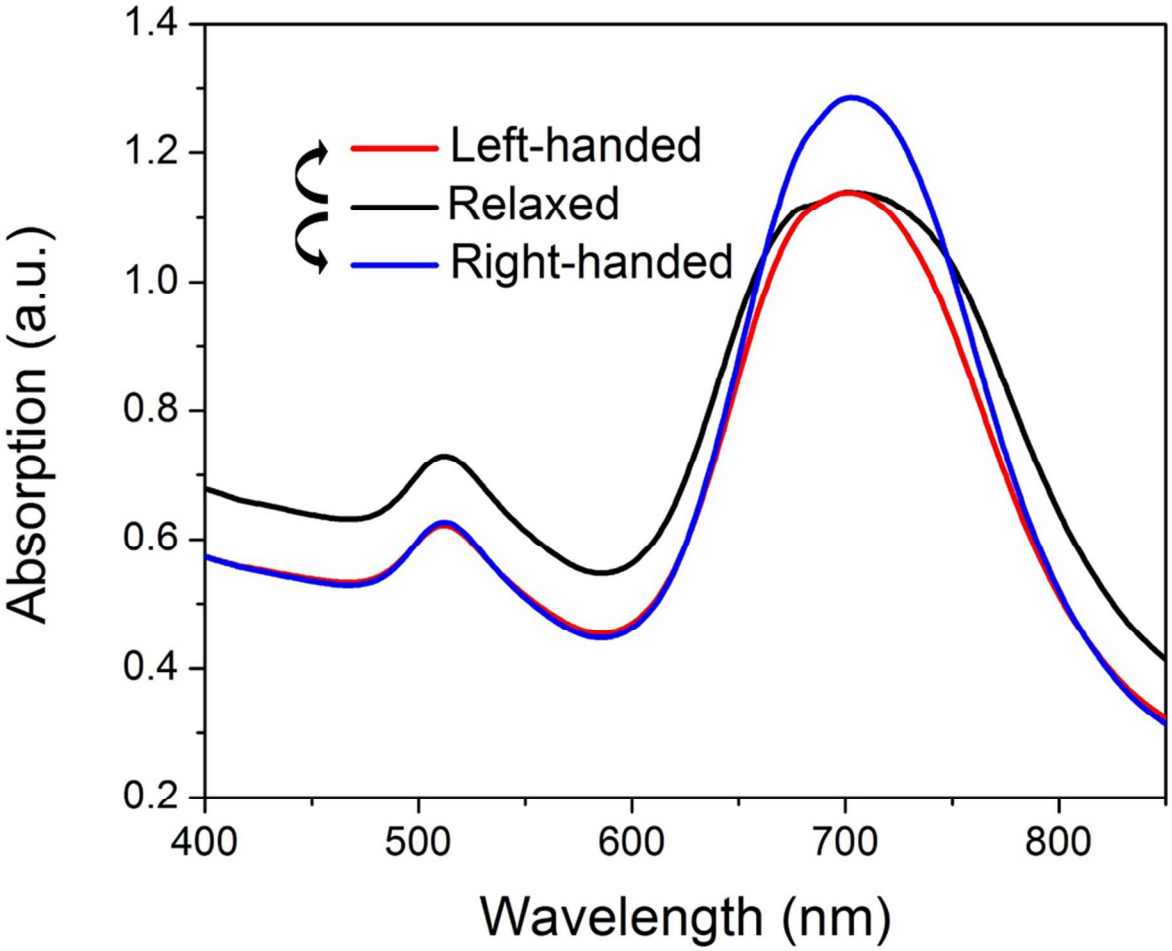

Figure S12. The experimental absorption spectra change after a single step reconfiguration of the AuNR superstructures from the relaxed state to the left-handed and right-handed state. No apparent aggregation was observed from the absorption spectra.

Note S6. Theoretical discussions

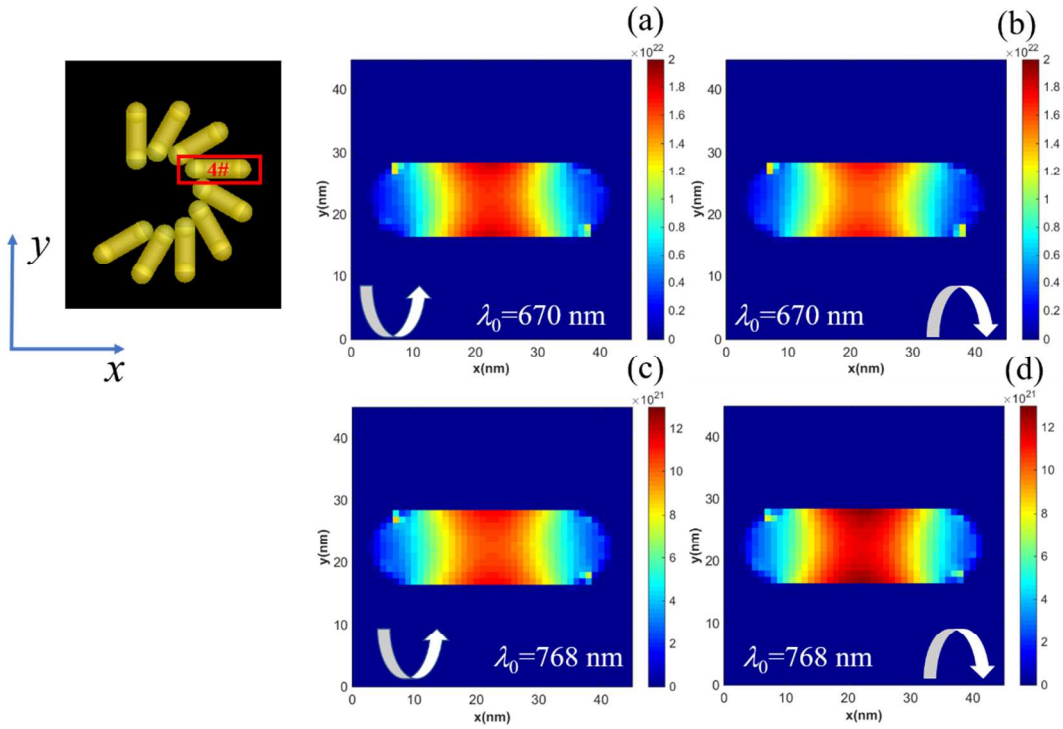

Figure S13. Power absorption maps (unit: W/m^3) of the 4# AuNR (inset on the top-left) within a chiral supra-structure at λ_0 = 670 nm (a, b) and λ_0 = 768 nm (c, d) under LCP (a, c) and RCP (b, d), respectively. The handedness of the polarization is labelled with a rotated arrow. The *x*-*y* cut plane passes halfway through the nanorod.

Figure S13 clearly shows the difference between the power absorption at the CD_{max} wavelength λ_0 = 670 nm (a, b) and CD_{min} wavelength λ_0 = 768 nm (c, d). CD spectra can be understood by the absorption differences between the LCP and RCP, with negligible contributions from scattering. In Figure S13, absorption per unit volume can be defined by the following equation[7]:

$$P_{abs}(\omega) = \frac{1}{2}\omega\,|E|^2\, imag[\varepsilon_{\mathrm{Au}}(\omega)] \quad ,$$

(2)

where ω, $|\boldsymbol{E}|$, and imag[$\varepsilon_{\mathrm{Au}}(\omega)$] denote angular frequency, amplitude of electric field, and an imaginary part of permittivity of gold. Note that the absorption difference of the individual nanorods in the *x*-*y* plane (e.g. a, b) only takes up a small percentage of the overall extinction difference, therefore the strong CD spectra are obtained due to the volume integral within the entire superstructures. Additionally, the induced surface current mostly flows along the *x*-axis, which enables the absorption to be dominant along the *x*-axis.

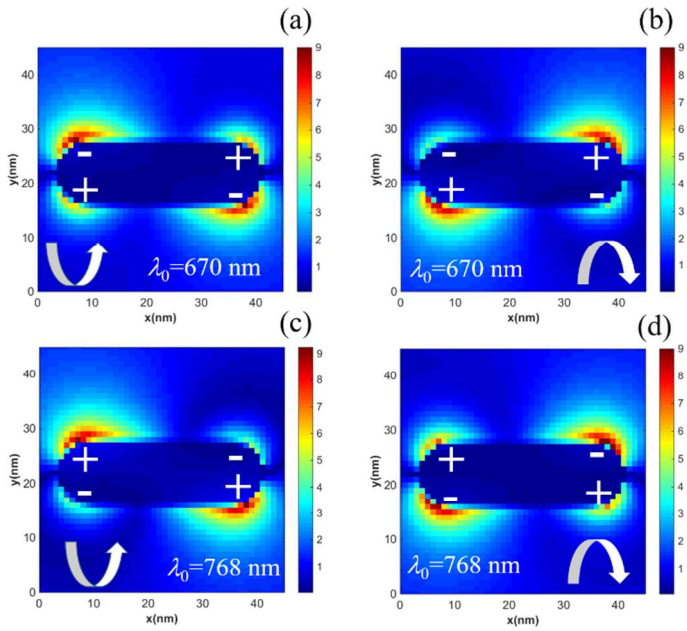

Figure S14. $|\boldsymbol{E}_y|$ field maps of the 4# AuNR (inset on the top-left in Figure S13) at λ_0 = 670 nm (a, b) and λ_0 = 768 nm (c, d) under LCP (a, c) and RCP (b, d), respectively. The map scale bar is normalized with the source intensity. The handedness of the incident polarizations are labelled with a rotated arrow. The *x*-*y* cross-section passes halfway through the nanorod. The '+' and '-' signs denote the positive and negative values of the real ($\boldsymbol{E}_y$).

In order to analyze the electromagnetic mode that was oscillating in the individual AuNR, $|\boldsymbol{E}_y|$ field profiles were calculated as shown in Figure S14. $|\boldsymbol{E}_y|$ fields were the main components of the E-fields, which were the signature of the evanescent wave (along the *x*-axis) and the oscillating plasmonic modes. The direction of the fields was evaluated with the real ($\boldsymbol{E}_y$) (denoted by the sign '+' or '-' in Figure S14). When comparing Figure S14 a&b at the wavelength of 670 nm (CD_{max}), it is evident that chiral field patterns had been generated. The stronger source-induced net dipole moment was along the *x*-axis in Figure S14a by evaluating areas with $\boldsymbol{E}_y$ fields that had oppositely paired signs. Likewise, when a comparison was made between Figure S14 c&d at the wavelength of 768 nm (CD_{min}), the stronger net dipole moment was confirmed in Figure S14d. For dipole-light interactions, only the net dipole moment along the *x*-axis in the 4# AuNR was responsible for the coupling of the *x*-polarized component of the incident LCP or RCP. This coupling gave rise to the different absorption (CD effect). The stronger power absorption maps as shown in Figure S13 a&d, as compared to those in Figure S13 b&c, respectively, could be explained due to the coupling as well.

Note S7. DNA design and sequences

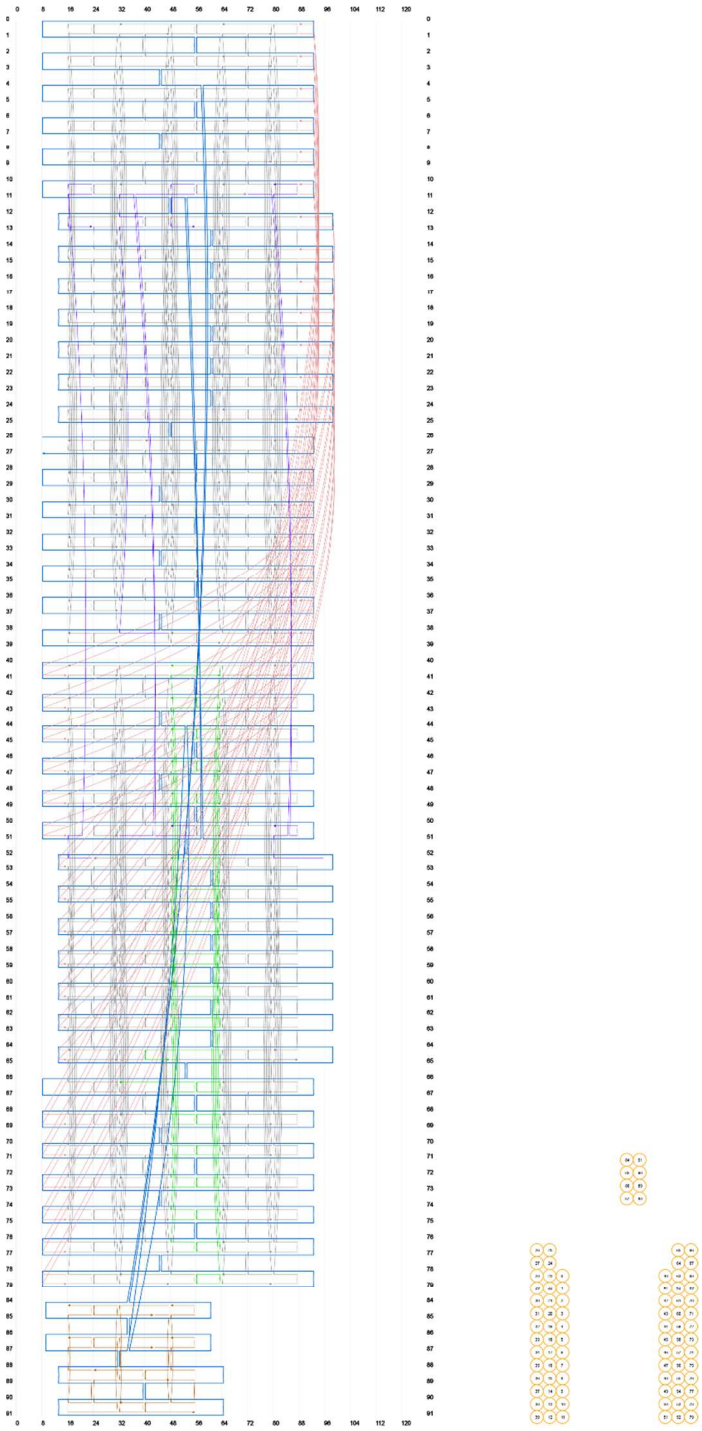

Figure S15. A strand diagram of the folded-state DNA origami. Inset at the bottom-right is the end view of the numbered DNA helices. The purple colored strands are the hinge strands that bridge the arm and the spacer. The green colored strands are the handle strands for the AuNR attachment. The brown colored strands are the helper strands for the 8 helix-bundle spacer. The red colored strands are the connector strands that were used for the hierarchical self-assembly.

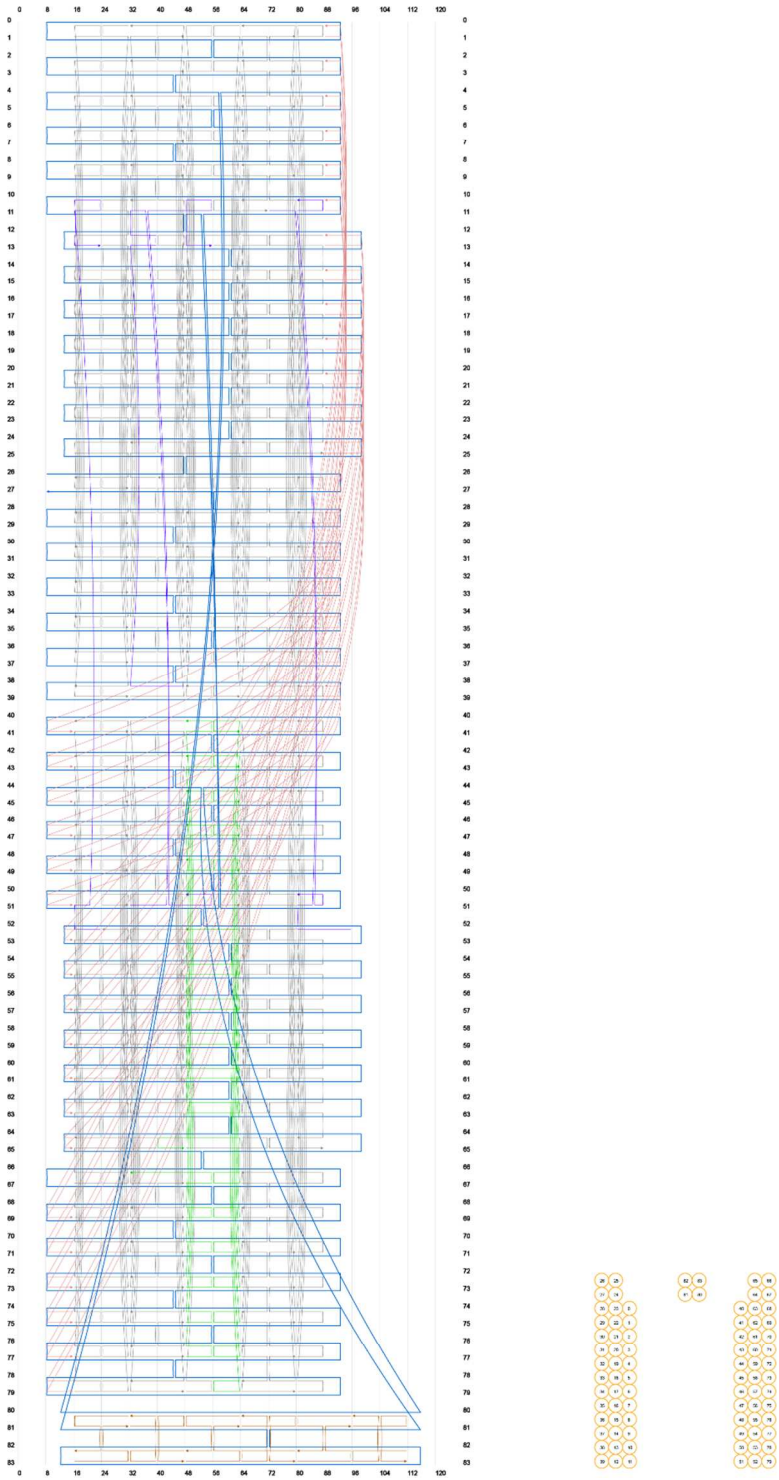

Figure S16. Strand diagram of the extended-state DNA origami. Inset at the bottom-right is the end view of the numbered DNA helices. The purple colored strands are the hinge strands bridging the arm and the spacer. The green colored strands are the handle strands for AuNR attachment. The brown colored strands are the helper strands for the 4 helix-bundle spacer. The red colored strands are the connector strands for the hierarchical self-assembly.

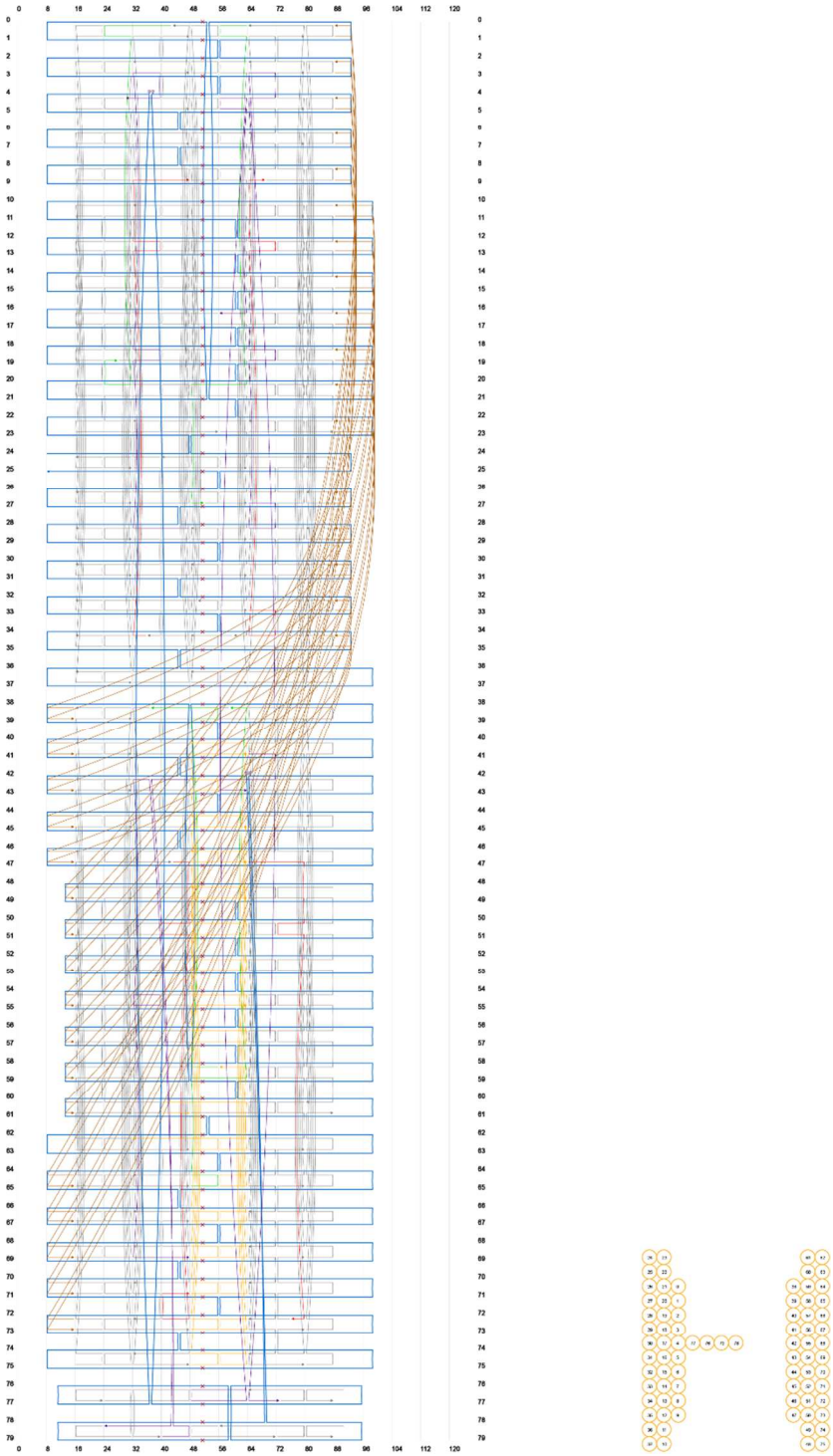

Figure S17. A strand diagram of the H-shaped DNA origami. Inset at the bottom-right is the end view of the numbered DNA helices. The red and green colored strands are the touching strands at the two ends, respectively. The purple colored strands are the hinge strands that bridge the arm and the spacer. The orange colored strands are the handle strands for AuNR attachment. The brown colored strands are the connector strands for hierarchical self-assembly.

DNA sequence for the capping strands that were modified on the surface of AuNRs:

5'- GTG AGT ATC TGG ACT GC/Thiol/-3'

Scaffold strand: home-made M13mp18

DNA sequences for the helper strands used in forming the V-shaped DNA origami (Figure 1B in the main text) and those of the lock and key strands used in the reconfiguration.

Function	**Sequence**
hinge	CCTGTAGCATTGCTGCGCAACTTCCGGAGGGGAAGATCGCGATTAA
hinge	GGGCGCATAAAAATCCAAT
hinge	TTTGTCGTAGTACAAAGCGCCCGCTTCTGCGCCAGCT
hinge	CCGTCGGATTCTCCGTTATGTCGTAACCGAGTTTGAG
hinge	CATAGAACTCAAACTAGGGGATGTGGGCGATCTTCAGCCACAGACAGGGGTCAGGGAT
handle	CCA GAT ACT CAC AGTTGATTCTGTAGCTTCAACCATCGCCCACGAAGAGAAGATTTTAGC
handle	CCA GAT ACT CAC ATTTTAAGATATTTTCAAATACGTAATGCGCTAACCGCCACATAATCA
handle	CCA GAT ACT CAC CCCTGTAATTAGCAAAATGTACAACGGAGATTTGTATCATCGAGGCGC
handle	CCA GAT ACT CAC TGGCTTAGCTCCAACAGCACAAAAGGAGCCTTTAAGAATAGATTAGGA
handle	CCA GAT ACT CAC CAAAAAGAGAGCAACAAAAAAAAAGGCTCTTAGTGTGATACTTTTTCA
handle	CCA GAT ACT CAC GAAGCAAATTAAGAGGCTGTTTCAACAGTTTCCCTCATTTAATAAGGC
handle	CCA GAT ACT CAC ATATAATGAACTGGCTAGCAGCGAAAGACTGGGCAGAGGCGCCAACGC
handle	CCA GAT ACT CAC CATAGTAAAGCTTAATGACAATGACAACAGAAAGTATAAAAACACCGG
handle	CCA GAT ACT CAC GGCGCGAGAGTAATCTGCGCGAAACAAAGTGTGGAGGTTGCCCTCAGA
handle	CCA GAT ACT CAC TCATCAAGTACGTCAATCATAAGGGAACCGAA
handle	CCA GAT ACT CAC TCAGAAGCTTAAACAGTTGACCGTAATCCCTC
handle	CCA GAT ACT CAC GCAAAGAACTGAAAAGCTACACTACGAAGGCATTCCAGTAAGGCAGGT
handle	CCA GAT ACT CAC GTTTAGCTCCCAATTCGTCAGCATCGGAACGACATCTTTTAGCGTCAT
connector	ACGTAACAATCGA
connector	AAATCCTCGGATT
connector	ATTATTCGTCACC
connector	ACATTTAACAAAAT
connector	TGATGGCAATTGAC
connector	AAATTTACATCGGG
connector	AATACGAACCGCC
connector	ACCACATTTTAAG
connector	CATTACGAGAGGG
connector	AAAACCAACCTTT
connector	GAGCAGTTTAATT
connector	TCTACGTTACGCA
connector	AGTGCCGTAAAAT
connector	CTATGCACGTAAAA
connector	AGGTATTCATTTCA
connector	TAATAAGTATCAA
connector	CATGACAACTAAT

connector	TAACAGTACCTGAC
connector	CAGCATATTCTGA
connector	CTTTCAATAGTGAA
connector	TGCATAATACTGC
connector	TGCTTCTGTAATTG
connector	TTGAGATGTGTAG
connector	CGCCATCAATATAA
connector	GAACCTATAATGA
connector	GGCAATTTAACGG
connector	CACTCAAGCTGCT
connector	CAGAGGCGAATGAG
connector	AAGAAAATAAAAC
connector	GTGTTTCATTTGAA
connector	TCAAAATTATTAAA
connector	GAAATCGTCGCTAT
connector	TTTGAATTAAAGC
connector	TAGCGTCCCTGCC
connector	GCTGAGAAGAGTCC
connector	GAAGCAATAGCGA
connector	ACTGAGTTTTACA
connector	CACCCTCAGTGGC
core	TCAACAGTTTCTTACCAAGCCCCATAAAATTCGGTCAGGACCAGACCG
core	CGAGGAAATAACGTCAGAAGCATAAAGTGACATAAAACAGTAATGCGC
core	ACATGGCTATTTACCGCCAACCTATATACCAATGACAAGAGCTGACCT
core	GAGTAGTAAATCATTGAGAGGCTTCGCTTTTGCCCCCTGCAGTATTAA
core	GCCACCACACCCTCAGGATAAATTGCCTGAGATGCGAACGCATATAAC
core	TTTTTGTTTATCAACACGTGCCAGCTGCACTTAACCTCAAACCGCCTG
core	AACAGTGCCCGTATGCGGGTAGCAAACGGGTAATTGAAACACCAGAAC
core	CAAATGCTAAAGCGGATTTGCTAAACAACTAGCGAGAAAAATCTTAGG
core	TGTTTTTATCCATCACAGGTCGACTCACGACGGAGTTAAGGCCAGCTT
core	AAATGTTTCATAAATATCTAAAGT
core	GCCGCTACCACCACACCAACGCGCAGACGGGCTTGAAGCCGAACCTCC
core	GAACTAACAAGAAAAATTAAAGGCTGAGGACTGGTCAGTGTGTACTGG
core	TTACCAGATGCAAAAGAAAGGAACGTAAATGAACCCATGTCTACAACG
core	AGAGTCTGTAATCAGTTAATCATGACGAGCCGAAAATGAAGAAACGAT
core	TTCCTTATAACAAGAATTGTTAATGAATCGGCCCGCCGCGATATCTTT
core	CAACAGTGGCAGAAGAAACATCAAAAACAGTATAACGGAAGATAGCCG
core	CAAACGTACGCAATAACATGAGCTCGAATTCGGAGGCCACAGGTGAGG
core	ACGTTGGGGGAACAACGGTCGCTGCAGCTTGACAGTACCAAGTATAGC
core	TCAGAGGGCAAGAATTTTGTAAAAGGCGAAAGTCGGCCTTCCATTGCA
core	GTTTAAACAGTTAATGCGGGATCGATATATTCATTATTACAGGTATGA
core	TAATAGTACATCCAATGGGTGAGATATTTTAA
core	TAAGAGCATACCAGAAATCCCCGGGTACCAAATTAGTCTTGAGATAGA

core	AAATATCGCGAGCTTCGCTCATTTAACGTTAAAAAAGCCTATATGCGT
core	CCAACATGGGAACCAGAGGTCATTAATGCCGGAAATGGTCAATTCTAC
core	TAAATCCTTACAAACAATGGAAGGGCGTAGATGAACGGGTGGCTGTCT
core	ACAGGAAAAACGCTCAGTTGGGAAGCTGCAAGGCACTCCACCCAATAA
core	TATTATTTTGCCAGTTCTCACTGCCGTATTGGTGTAGCGGAGCGGGCG
core	TCTAAGAAAGATATAGGCCCCAGCGGGTTGAGCTACGTGAGAAAAACC
core	AGAACTGGACTCCTTAAATTAATTATTACCTGAGAGCCAGAAAATCTA
core	GGAATCGTAGACTGGAAGACGTTAAACTAAAGACCCTCAGAGTACCGC
core	TTGTCATTGAAAATACGAATAAAGCCTGGGGTGTATTAACCTTAATGC
core	AAGTACCGGAACAAGCCTACCATATCCTGATTACGTTATTGTTTGAGT
core	TTAGCGGGGACTCCTCCATAACCGTCACCCTCCATTATACCTTATGCG
core	TGTACAGACTTTGAAACTGCTCCATGTTACTT
core	AATCATAATACCGACCAATTTTTGTGGCCTTCAAGCCCGATATTATAG
core	AACCACCACCACGCTGAGCAAAAGAAGTTACAACGGAATATCCCATCC
core	GCGGAATTGGAACAAAACTCGTAT
core	AGCAAGCCGCCACCACAGCGGAGTAAATCTCCCTATCATATTACGAGG
core	CCGGAATAGGTGTAAATAATTGTAGTTGCGCCTGCGAAAGATTCATCA
core	AAGCATCACAATATCTTAACGGATTCAGATGACAATAATCATTAAACC
core	TTCACCAGGACCTGAATTTCCCTTTGTGAGTGAGTAAGCATACCCAAA
core	CGGCTAAACAGGAGGCCACAACATGTCATAGCGAATTAACTGAACAAC
core	GCAGATACTTAGGAATTTCTTAAAAGGCTTGCAACATGAACTATTTCG
core	TTGGGTTATATAACTAGGGAACAACATCAACAACCCTGACAAGACTTC
core	TCCAGTTTGGAACAAGCAAAGGGCACCATCAC
core	CGACGGCCTTAGTAATACCGTTGT
core	CGCGTAACAGGGCGCGCAGTCGGGAGTGAGCTCCAAATAAAATAGCAG
core	AGACGTTTTGCGGGAGAAGCCTTTCCTGAGTAATTAAGCACAGGCAAG
core	TTGCCTGAGTAGATCTTTTCCCAGTCTAGAGGGGAACCCTGAACAAAG
core	TATACAAAAGGGCTTAGTACCCCGAGAGAATCTTTCATTCAGTAGATT
core	TCCGGCACATTCGCCAGGTGCGGGCCTCTTCGACCGCCAGGCTGGTAA
core	AAATCACCTAATTTAGAGCAAACAGTTGATAACAACATGTTTTGCGGA
core	TAGTTTGACATTTCGCAGAGGGTACCATCAATCCGCCACCCCAGAGCC
core	TTTATCAATGAAATGGTTGGCAGA
core	GAGGCTTTCGACGATACGAATAATCTTTCGAGTTGATATAGGCGGATA
core	ACGTGGCGAGAAAAGCGCCCTGAGTGATGGTGACCGCGCCCAATAGCA
core	AGATTAGTGAATCTTAGCGGTTTGCCGCTTTCTACTATGGTCGTTAGA
core	TAATTTACAAACCAATATATACAGCAGAAATAATAATACATAGAAGTA
core	TACCTTTATTGATAAGAAGATTGTAATCATATATTGAGAATAACAACG
core	TTAGACTTTTGCCCGAGTTTGGATATTCCTGATTATCAGA
core	CATTCAGTCCAAATCACACTCATCTCGAAATC
core	GAGCCGCCCCTCAGAGATGATATTATTCAAAAAAATCATAATAAAGCC
core	ATTAAGACTAATTAATAGCGTAAGACAGACAA
core	GTTTGAAATTACTAGATATTTTGTAAAACAGGAGGTCATTTTTAAATA
core	AGCCGGAACGCCTGATATAGGCTGACCGGATA

core	CATCGTAGCATTCCAATTTCCTTCACCGCCTGACTAACAAGGTGCCGT
core	ACCCTTCTTCACACGACATAGCGAGTCTGAGAGTGTAGAT
core	CTGACCAACCAGGCGCAAATTGTGTTTGACCCATATTCACAAAGCGCA
core	AGCGCATTGAGAGAATTCCGCTCATTAATTGCTGCTTTCCTTGCTTTG
core	AGGGGAAGGGAAGAAACACCAGTGGGGGAGAGCCAACGCTAACGAGAT
core	TGCAACTATCTGGAAGGATGAACGAGGCTATCAGCCACCACTCCCTCA
core	TCAACTTTAATTGGGCTTTTTCATAGAATACACAGAATGGAAACAAAT
core	TTTATCCTTGCTATTTGGGTGGTTGTCCACGCCGGGGAAAGGGAGCCC
core	AAAGCACTAGTTTTTTAAATCAAAATTAAAGACAGAAGGA
core	TATTTTTGAGCCCTAATTTAATGGGAAAACAATTACGCAGAGGTGGCA
core	ATCAGAGCGGGAGTCAGCCTAATGAAACCTGTATAGCGTCTTTCCAGA
core	CAGACGATTGGCCTTGCCAGCGATAAACGAAACTTGCCCTGACGATGG
core	CCCTCAGACAATAGGAATTTTCTGCGTAACGATTCATTGAATCCCCCT
core	ATAACCCATAATTGAGAAGCTTGCGTGTGAAACCAGAATCGGGATTTT
core	TTAGAGCCAGGAAGGTGTTTAACGTCGCCTGAAAATAATAAGTTTATT
core	CCAAATCAAAATCGGAATCCTGTTAGAGTTGCGTTTTAGCTTAAATCA
core	CGCAAGACTTAGTTAATTCGCGTCTTAAATCAAAAGCGAATTAGAGAG
core	TTGACGCTCAATCGTCAATCATAGTAGCTTAGGGGACGACCAATAGCT
core	TCCAACGTAGTCCACTAGAATAGC
core	CGACTTGCGAATCATTGTTCCGAAATCGGATAATTCGACACTAATAGA
core	ATGCAATGATTTCAACACCAAAAACATTATGA
core	GCCTAATTATCCCAATAACTCACACAATTCCACGATTAAACTGAGAAG
core	TGACAAAATCCCTTATGGGGTCGAGAAACCACACGTGGAC
core	AACATTATCATTTTGCATCATCATTATACTTC
core	GTTATCACCGTACTCACACGTTGAGAGAATAGAAGTTTTGCCAGACAT
core	ACATATAAAAGACACCAAATCGCGAGAAACAAGGTCAGTTCAGTTGAA
core	CCTTTACAAGACGGGATGTTTCCTATGCCTGCGCAAATTAAACATCAC
core	GAACTGATAATGGCTATCAATATAAGAATCCTTGAAATAGGACAGTAT
core	GTTGGAAACCAGTAATCCTACATT
core	AGGAATTGGTCAATAGAAGAAATTGTTAGAACAAGCCGTTTTTATTTT
core	GTTGAGATATAACGCCTCAGCTTGAATTTTTTGGAGGTTTAACCGCCA
core	GACCATAAAGGTCTTTTTAAATGTAAAAATAATTTCATCTATTTAATG
core	TCAGAGCATCGGTTGTGCAAGGAT
core	TTCATTACGAATAAGGGAGGCAAAGAGGAAGTTACAGGAGCCTTGAGT
core	GAGGCTGAGTTTTGCTTACCGATATCGGTTTAAAAAGGAAACCCTCGT
core	ATAGTTAGTATGGGATTTGGGGGGTAATAGTA
core	GCCGCCAGCATTGACAAGGTAAAGCAACCGTTGTGGCATCAATAACCT
core	AAGTCCTGGGGAGGTTAACAGCTGATTGCCAGTATCTAAAATATCAAA
core	AACAAAGTAGAAACAATGAGTAACGCCAGGGTGGCCAACACGAGTAAA
core	AATATATTAAAGAACGCCAGCTTTACGGCGGATTCAGAAAACGAGAAT
core	ATCTTACCTTAAGAAAAATAACCTTTACCTTTAACATCGCACCGAACG
core	CGGCCTCATCACGTTGGACTACCTTTTTAACCTGGAAATAAAAAGGGA
core	AGCAAATCCGCGAGGCAGCAAGCGTTTCTTTTGCGAAAGGTCACGCTG

core	GTCTCTGATTTGATGATTCCATTAACGGCTACTGAATTACCAGTCAGG
core	CCGAGATAAGGCGAAAACCCTAAAGCCGGCGA
core	CCCTCAATCCTTGCTGTGAATACCAAGATGATATACATAATATGTTAG

L1	GCGGTCGTGACA TAGCGTCATAGCGACAACAATAAAAGCTAATG
L1	TCAGTACTCACG CCATTAGCAAGGCCGGTCAATAGAAAAAGGGCGACTGTCCAGA
L1	CAGTCAGCATTA AATTATCAGACGGAAATGAGGGAG
L1	GTTACATGTTCG CCGACTTGCAGTAGCACCAAAGACAAATTCAT
L1	TCCTACCTGAGG GGTAAAGTAATTCATTGGGAATTATAGCCCCCTAAAGGTG
L1	AGTACTTTCAGA CAGAACGCGCCTGCAAAAACGTCAGAGCCAGC
L1	GTTTCTACCTCA CGACGGAATCAAGCCAATGAAACCATCGA
L1	TAACATCCGTCT AGTAATTCGGTCATTTGCCTT
L1	GATAGGTCTAAT TCGGCATTTAAGAGAACGACAAAA
L1	TCTTTGGCGGAT AAAATCACAGCCATTTCAACCGATTTATTCATTTATTCGAGCC

K1	CAT TAG CTT TTA TTG TTG TCG CTA TGA CGC TAT GTC ACG ACC GC
K1	TCT GGA CAG TCG CCC TTT TTC TAT TGA CCG GCC TTG CTA ATG GCG TGA GTA CTG A
K1	CTC CCT CAT TTC CGT CTG ATA ATT TAA TGC TGA CTG
K1	ATG AAT TTG TCT TTG GTG CTA CTG CAA GTC GGC GAA CAT GTA AC
K1	CAC CTT TAG GGG GCT ATA ATT CCC AAT GAA TTA CTT TAC CCC TCA GGT AGG A
K1	GCT GGC TCT GAC GTT TTT GCA GGC GCG TTC TGT CTG AAA GTA CT
K1	TCG ATG GTT TCA TTG GCT TGA TTC CGT CGT GAG GTA GAA AC
K1	AAG GCA AAT GAC CGA ATT ACT AGA CGG ATG TTA
K1	TTT TGT CGT TCT CTT AAA TGC CGA ATT AGA CCT ATC
K1	GGC TCG AAT AAA TGA ATA AAT CGG TTG AAA TGG CTG TGA TTT TAT CCG CCA AAG A

L2	TACAACGGTTAT TGACGGAAATTATTCAGGAATTAGCATGTTCA
L2	GCCTAGAATTAC TGTCCAGACGACGACAAAGACAAAGTAAATAT
L2	ATAGCCCAGTAT TTTCGGTCATAGCCCCAGCCAGTAATCGATAG
L2	GCGTTGAACGCT TGGTTTACCAGCGCCAATAAACAAAGCCAGCA
L2	ACTCTTGTAGTT CGACTTGAGCCATTTGTTAAAGGTAATTCATA
L2	TTTCTCTACAGC AGCGTCAGGATTGAGGCATTACCAAGTAATTC
L2	AATCATGAGTGC ATATAAAGTACCGACAGCGTTTTCTTGCCTTT
L2	AGCGGTCTTACG GCCGGAAACGTCACCAAATCAAGTATCGGCAT
L2	GCGTGACACTCC TAATCAGTAGCGACAGATGAAACCATAAGAGA
L2	TCAATCGCATGT AAATCACCAGTAGCACGAGGGAAGAGGGCGAC
L2	AACGACGAGCAG GCTAATGCAGAACGCGCAATAGAAGAATTATC

L2	GCGAATAATACC ATTCAACCACTGTAGCAAAGGTAATTAGCAAG

K2	TGA ACA TGC TAA TTC CTG AAT AAT TTC CGT CAA TAA CCG TTG TA
K2	ATA TTT ACT TTG TCT TTG TCG TCG TCT GGA CAG TAA TTC TAG GC
K2	CTA TCG ATT ACT GGC TGG GGC TAT GAC CGA AAA TAC TGG GCT AT
K2	TGC TGG CTT TGT TTA TTG GCG CTG GTA AAC CAA GCG TTC AAC GC
K2	TAT GAA TTA CCT TTA ACA AAT GGC TCA AGT CGA ACT ACA AGA GT
K2	GAA TTA CTT GGT AAT GCC TCA ATC CTG ACG CTG CTG TAG AGA AA
K2	AAA GGC AAG AAA ACG CTG TCG GTA CTT TAT ATG CAC TCA TGA TT
K2	ATG CCG ATA CTT GAT TTG GTG ACG TTT CCG GCC GTA AGA CCG CT
K2	TCT CTT ATG GTT TCA TCT GTC GCT ACT GAT TAG GAG TGT CAC GC
K2	GTC GCC CTC TTC CCT CGT GCT ACT GGT GAT TTA CAT GCG ATT GA
K2	GAT AAT TCT TCT ATT GCG CGT TCT GCA TTA GCC TGC TCG TCG TT
K2	CTT GCT AAT TAC CTT TGC TAC AGT GGT TGA ATG GTA TTA TTC GC

DNA sequences of the helper strands used in forming the H-shaped DNA origami (Figure 5 in the main text) and those of the touch strands, block and release strands used in the reconfiguration.

Function	**Sequence**
hinge	ATATCAAATGTTTGGAGTAAATCGTTAAGACGGTTTGCGTTCGGCCAAAGATAGCCG
hinge	ATGAAAAGAGTCTGTCCACCCAGCACCTCCCGATAATAAGCTTACCCTCAGGAA
hinge	GGATTGACCAGCTTTAAGTTCGAGCTAAAAGATTATGGCTTTTGATGAAG
hinge	ACGTAGCAAAATTCATCAACATTAAATGTG
hinge	GAACTTAGGTCACGTTTAAGAAAAGTAAGCCGCGCGGGTTGCGCTCGTTCACTC
hinge	AGTTTATTAAAATAATTCGGCAACATATATATTTTG
handle	CCA GAT ACT CAC CGAAAGAGACTAAAGATCGCACCATTACCATTAGCAAGGGAATCAAG
handle	CCA GAT ACT CAC CCCTGCCGGAACAATATTATAGTCAGGGCAAACGTTAGTCAATCA
handle	CCA GAT ACT CAC GCCCAATATAGTACCGCTAATGCAGATACAT
handle	CCA GAT ACT CAC GGAGGTTGGAACCCAAAACCAAAATAAAA
handle	CCA GAT ACT CAC CGTAACATATTTCGTCGTCATAAATATGACGATGAACCGGAGAGG
handle	CCA GAT ACT CAC TCACAAACGCTGAGCTTAATTGCTGAGGGAACCGATTACGGAATA
handle	CCA GAT ACT CAC GAATTGCCAAATAAAACCAGACCGGAATC
handle	CCA GAT ACT CAC TATTCGGTGAGGTGAATTCAGCAAACTCCAAAGACACCGGGCGCG
handle	CCA GAT ACT CAC AATAGAAACGTCTTTCTTGTTCATTGAATCCCTAGCATGAGAAGC
handle	CCA GAT ACT CAC CTTTGAGGTAAAGGCCTAAATATA
handle	CCA GAT ACT CAC TTGCTTTCGAATAATATAAAAGCAAAGCGGATTTGCGGAAAAGAA
handle	CCA GAT ACT CAC AAATCACGCACCTTTAGCGTCAGACTGTAG
handle	CCA GAT ACT CAC AGTTTTGTCTGAGTTTATAGCGAGAGGCTTTTTAATGCGGTAATC
connector	GCATAGTATCATAT
connector	AATCCAATCGCTGA

connector	GACGAGAGACTACC
connector	ACGAGTACATAAAT
connector	CATAAAGCATCAT
connector	TGGCATTAACATC
connector	ATCATAGGTCTTTC
connector	CGCCACCCCCACG
connector	TAGTAGCAATTCA
connector	GAAAAGACAAAGAA
connector	CTCTGAATCGTGC
connector	CCTGTTTACCGTT
connector	TCGTGATGAAACAA
connector	AAAAGCCTGTTACA
connector	ACAGTCAAAGGAA
connector	AATTGATCACCAT
connector	TTAATGGAAACGTG
connector	CCATTAGAAATAA
connector	GATCCGACTCCTC
connector	TAAAAATACCGACC
connector	TTAATGGTTTGAAT
connector	ACATTTAAATCGG
connector	ACAGATACATTTC
connector	GTTTTGACAGGAG
connector	ATTTGTATATTTT
connector	CCAGCATTTCTTT
connector	TTCCCTTAGAATTT
connector	GCGGTTCAGAACC
connector	ACGGGGTCAGCAT
connector	GCAAAAGAAGAATA
connector	GAGGCTGACCGGG
connector	CCTTCCTTGAAAAC
connector	CCGGAAGTGCCTT
connector	AACCCTCAAGGAT
core	TCGGGAAACAGCTGCATTATCAAAATAGCGATTCAGATGATCAATATA
core	AAAATATCCGTCAATAAACTTTTTTGTAAATGAAGCCTGGCTTTCCAG
core	CTTCTGGTACTCCAGCATAGCAAGGAGGTTTTCTTTGATTAAATTAAC
core	GAGATTTAGGAATACCCGGAACAATTTTCAGGGTACAAAC
core	TCCAACGTAGTCCACTATAAATCA
core	CGAACTAAACATTCAACCACCCTCAGAACCGC
core	TTAAAATTTAAATTGTTTGCCCTGTTTAATCACAGACGTTCGATCTAA
core	GAAATTGGCTAACTAACCAAGTACCGATAAATTCGACACTAATAG
core	GTAAAGATTCAAAAGGGTCCAATAAAGTTTTGTTAGCGGGGTTTTTAC
core	GAATGGAACGTCATACAAGAGGAACAAAAATCGGATAAAATGCCTGAG
core	CAGAGATAATAAAAGGTATCCCATGGGTATTACACCATTCGCCATTCA

core	ATTAGACTTTTAAAAGCTCCGGCTTAGTGAATTTAATGAAATTGGGCG
core	TATCGGCCGCCTGAGTTTTAGCGATACAATTTAAAGTCAGGAATTAAC
core	TAGAATCAGGGATTTTCCAAATAATTTCCAGAAGACGGGAAGGGTAAT
core	CCAGTGCCTGTTTCATAAGTCCTGAATAGCACT
core	TTACTAGAGTGTGATATTGAAAGGGGTTATCT
core	AAAGAATAATCCCAATAGACAGGATAATCAGT
core	CACCCTCACACCCTCACATTATTACGTTGGGAGATCTACAAGAGTCTG
core	ATCATATTACCACCAGAGAGTCAATAGGTTGGACTGCCCGGGTGCCTA
core	CGGATAAGGGAATAGGACGAGGCATAGTAAGA
core	AACAGGGACCTTTACATATTATTTGCCCGAGAAACGTGCTGAAAAACC
core	AGCTGAAACTATATTTAGCTCAACAGTTGATTAGAGCCACCATAATCA
core	GTTGAGGCAGCCGCCGGATAAGAGACTAAAGTGCAAATGGTAGTTTGA
core	ACCACCAGAGGTCAGAAGTACCTTCGTTTTAACAATAAAGAAAACATT
core	AATCTCCACTTTAATTAGAACCGGACCAGGCGATCAATAGGCCAAAGA
core	GCAGAGGCGAATACCAGATGAATA
core	GATTGCCCGAGAGGCGCTGAACGCGAGGCGTAGAAGAACTGAATA
core	GTAAAGTAAATGAATTTTCTTTTCAACACACCAGAATAACAAAGATTTTTGTAATAGGAA
core	ACGGAGATTCATCTTTAGGCACCAACCTAAAA
core	GATCGCGCCGGAAATATTTTCATTATCATTCAATCGTCAGTCACACGACCAGTAGAAC
core	AGCGAGTAGGATTCTCCGTGGGAAATCGTAACCGTGCATCAGGGGACG
core	CGGGCCTCAACTGTTGGTCTTTCCTCGTAGGACAACAGGAGAACAATA
core	GAGTAACAAAGTTTTACCATAAATGCCCGAAATTGTACCACCTCAGAG
core	CATACGAGAAAGTGTACTGATGCATTTTTAACTTTGAGTATTTGCGGA
core	CAAATATTCGCATTAACTGCTCATTCTTGACAGTATCGGTACAGCTTG
core	TAAAGCCAACGCTCAGAGGCGGTATCAAA
core	CACCCTCACGAGGGTAATCCGCGAAAAGTACA
core	AAGATAAAACAGAGGTACAGTAGGCCAGTAAT
core	AACGCCAACGACGATAATGGCTCAGTACCAGG
core	CTGCAGGTCGACTCTAGAGTACCGAGCACCTAAATCGCGAGAAGATAATACTTAGAAGT
core	CTGTTTAGAGGTGGCATGCGGATGGATTAGAGCGATTGGCTAAAGCCA
core	TTTGCATCACGCAGTAATAA
core	CATCACTTTTGCTGGTATATAGAAGCCGTTTTCCAGGCAAAGCGCATT
core	CCAGTAAGAGCGCAGTAAATATCGTAATTGCTCAATAAATACTAATAG
core	AACATCTGGTCAGTTGGCAACTTGCTGAAACACCGGTACCAGTA
core	ATCGAGATCCTTTGCTCAAAC
core	TGAACACGATTGTTTTTTGGTGGTTCTTATAACGTCAAACCTACC
core	ATACCGATACCATCGCTTTGAAAGGAACGAGGGGAAATTACGTCACCGACTTGAGC
core	TGCAGCAACTGGTTTGTACCTTTTACATCAAGTTTACATCATAACGGA
core	CTTTATTTGTAATACTTTGCATCATCAAAGCGATCCTCATCTTGATAT
core	TGAGCGCTTAAGCCCAACTTGCGGCAAATCAGAATATCCAAAAACGCT
core	AAGAGAAGAGTATTAAGTTTAGACGAAAACGAAAATGCAAATTTTTAG
core	ACAAAGAACCTGATTAAGCTTAGATCGCTATTGAGACGGGGAGAGAGT
core	TAATGTGTAGGTAAAACCCTCAAAACCCTGACCTAATACAGGAGTGTA

core	ATCCTGATATTATTTGGTGAGTGAATTTGAATCCCCAGCAGGCGAAAA
core	TATAGCCCTGCCGTCGCTATCATAGGTAATAGCAATATGAGGCCGGAG
core	CCCAATGCGCGAACTGTTTTCGAGGCTTAATT
core	GAACGCATATAACATGTTTTACCACCCTCAGAGCTGC
core	GCCACCCTCTCAGAGCTCTGGAAGTGAAACCA
core	CTCCTTATTACATAAAGGTGCGTCTGGCCTTC
core	GGCTGCGCTTCGCTATACGAGCATAACGCGCCCTGACCTGTTTGAATG
core	TTACCAGAAAGGAATTTGTATCACCGTACTCA
core	CCAGGGTGTCACCAGTAATTAATTCAATATATCACGTAAAAGAAATTG
core	CAAGGCAAAGAATCAACAGGTCAGGCTTAGAGGCTCGCCACCAGAACC
core	AATTGCGAATAGCACGGTATTCTAAGAGAAAGGAGCGCCCGAACG
core	GCTATTAGTCTTTTCAAGGTAAAGAACAATAGCTGGAAAGGGGGATGT
core	AATTTAGGACGACAATACAATATTAAAGCGTA
core	CCGCCTCCCAGAGCCAAATATGCAGTCATTTTTCAATTCTCATACAGG
core	CATTTGGGGATAAATTGTCAATCAGCTTTTGCAACCGATA
core	TTAGAGGAGGCCGATTAAAGAGCGGGAAATCCCTTATTAAAGAAAATCGC
core	TACAACGCCTCATAGTTTAAGAACATGGTTTATAATCAGATGTATAAG
core	TATGTACCAAGAGAATATTACCTTCTACGTTACGTCACCAGATAGCAA
core	GTATTACATTTTGACGCTCCAAGAACCCTAATTTTACGCCAGCTGGCTGT
core	AAGAGAATATAAATAACCTCAAATCAGTATT
core	CTGGTAATGTGCCCGTACAGTTCATGGATAGCGTGAGAAATATTCAACCGTTCTAGCTG
core	AATTGAGTAATATCAGATTAGTTGTGCCAGTTTGTTTTTAACGGTACG
core	ACGACAGTATCGGCGAAGCCCTTTTGGTGTAGATGGGCGCCAAACGGC
core	CCTTATTACATCGGCAGCAGCACCGTAATCAG
core	ACAATGACCTGAACTATCCTGAATCTTCTTTATACTTGAATTATC
core	AACGCAATAATTTACCAGA
core	GCGTTATAGTGCCACGAAATCTAA
core	TTTGAAAGAATACACTAAAACACTTGTATCACTTTTTCATACAGAGG
core	GAGGAGGGAGGGAAGGTAACGACATTCAACCGAACGGCTGACCTTTCTTAATTATCAGC
core	TAGCGACACCGGAAACCATCTTTTCACCGGAA
core	TTCGCCTGATTGCTTTGAATTATTATTAATTA
core	GTTTTCCCGCGATTAATAATGCAGGTAGAAACGATTCACCTGAAATGG
core	TAGAAAATACATACGCAGT
core	TTATTAATTTACAAACTAACTATACAAATATATCACAATTGTAATCAT
core	TACAGTAATTCAGGTTACAATTTCATAACCTTCTGGCCCTCAACAGCT
core	ATGACCCTCAACGCAAAGGTCTTTTGCTTTAAATAAACAGTATTCTGA
core	CGCCATCATTGTCACACATAGGCTTGACCAACCCACGCATGGGATCGT
core	CATGGAAATACCTAAAACAAGCAAGGCTTATCATAGCTATAGCAAGAA
core	GAGCAAACCCGGTTGAATTTCAACACGAGAAAGTTTCAGCACGTTGAA
core	CGCGTTTTGCGTTTGCGTCACCAATTTCATTCAGTAGATTTCAATAAC
core	GCTGCAAGAGTCACGATCCAGACGCAGAGGCAATAGCCCTACCAGCAG
core	AACAAAGAACGGAATACCCAAAA
core	GAGAATCGCCATATTTAACGAACCAAAACATC

core	GAGGCCACCGAGTGAACGAGCGTCGAAACGATTAACG
core	ATGAGTGATTATCCGCTTTCAAGAAAAATAAGACATTCAACTC
core	TTTCCATTCACTACGAGACCCCCA
core	TCCAGTTTGGAACAAGCAAAGGGCTTCCTCGT
core	AGCATCACATCAACAGAATAAGGCATCTTCTGTCGAATTCCCACACAA
core	AACATGAAGATTAGGACCAGAGGGACCCTCGT
core	CTGTAGCCGTAATGGGAGGCATGATTAAGA
core	CGTAGATTCAGTACCTAAAACAAACATTTCAATTACCTGA
core	AACACCGCCTGCAACACAAATTCTAATCATAA
core	CAAAAGGGATATTGACCGCAGACGGTGTCGAAGCAACGGCTGAGGAAG
core	GGTCATAGCAAGCTTGAGAAGTACCGACAAAATCAATATGGCCAA
core	AAGAGTAATCAGTGAAATTTTTTCGGAGTGAG
core	CATCGAAATCGGCAAGCTAAACAGTTACAACGTGGAC

VL-touch	ATTAGAGCTTTAGGAGTTAATTTCGTTAAATACATGC GCAA GACGGTCCAC TGTTGCGAAG
VL-touch	GTG GAC CGT CTT GC GTAGCTATTTTTGAGAAGAAAAATATGCGATTTAGC
VL-touch	CCTTTGTTTATCTAATTCTGCGTTGTAAAACGACGG GCAA GACGGTCCAC TGTTGCGAAG
VL-touch	GTG GAC CGT CTT GC ATAAATGCAAAAGCTGCGGAAGAACCTATTTAATGCC
B1	GGCCACGCTCGG C TTC GCA ACA GTG GAC CGT C
R1	T CCA CTG TTG CGA AGC CGA GCG TGG CC

VR-touch	ATGCTGTTCATTTGCCAGCAACCCAATTCTGCTTT GGCT CGCGACGGAC TCGATGTCGA
VR-touch	GTC CGT CGC GAG CC TTTTCCTGTTTTTCACCGCGCTTACCAACGCTAAGGG
VR-touch	AGGGAGTCGGAACCAATCACCAGTAGCCTAATTATTT GGCT CGCGACGGAC TCGATGTCGA
VR-touch	GTC CGT CGC GAG CC TTTTCAAAAATGAAAATAGCAGAGCGCATTGCCTAATTCTAT
B2	CTAAGACGGCGT T CGA CAT CGA GTC CGT CGC G
R2	C GGA CTC GAT GTC GAA CGC CGT CTT AG

References

(1) Lan, X.; Su, Z.; Zhou, Y.; Meyer, T.; Ke, Y.; Wang, Q.; Chiu, W.; Liu, N.; Zou, S.; Yan, H.; Liu, Y. *Angew. Chem. Int. Ed.* **2017**, *56*, 14632-14636.
(2) W. Yu, and R. Mittra, "A conformal finite difference time domain technique for modeling curved dielectric surfaces," *IEEE Microw. Wirel. Compon. Lett.* **2001**, *11*, 25-27.
(3) A. Kuzyk, R. Schreiber, H. Zhang, A. O. Govorov, T. Liedl, and N. Liu, "Reconfigurable 3D plasmonic metamolecules," *Nat. Mater*. **2014**, *13*, 862-866.
(4) P. B. Johnson, and R. W. Christy, "Optical constants of the noble metals," *Phys. Rev. B*. **1972**, *6*, 4370-4379.
(5) S. A. Maier, *Plasmonics: Fundamentals and Applications* (Springer: New York, 2007).
(6) Gerling, T.; Wagenbauer, K. F.; Neuner, A. M.; Dietz, H. *Science* **2015**, *347*, 1446-1452.
(7) L. Novotny, and B. Hecht, *Principles of nano-optics* (Cambridge university press, 2012).